Gaussian Process Based Prognosis Model for Bridge Scour

Rajesh Kumar Neerukatti, Masoud Yekani Fard, Inho Kim, Aditi Chattopadhyay
School for Engineering of Matter, Transport & Energy
Arizona State University
Tempe, AZ- 85287, USA

Abstract— **Scour is one of the primary causes for bridge failures and therefore, a reliable prognostic framework is essential to prevent catastrophic failure. In the U.S., scour accounts for almost 60% of bridge failures. Currently available techniques in the literature for predicting scour are mostly based on empirical equations and deterministic regression models such as Neural Networks and Support Vector Machines and are designed to predict the maximum possible scour depth for a given set of flow conditions. In this paper RFID (Radio Frequency IDentification) sensors were used to measure the scour depth and we investigate the use of Gaussian process model. This model includes Bayesian uncertainty for prediction of time-dependent scour evolution based on the measurements from RFID sensors and pressure transducer. The evolution of scour under different flow conditions was studied. The model was validated with the experimental data conducted in four different flumes in different conditions and field data in different test locations. The robustness of the algorithm was also demonstrated under different scenarios, such as lack of training data and equilibrium scour conditions. The effects of initialization of hyperparamters and the use of different kernel functions on the predictive capability of the algorithm were investigated. The results indicate that the algorithm is able to predict the scour evolution in both laboratory and field conditions with an error of 5% or less given enough training data.**

Keywords—scour prediction; Gaussian process; data analysis; data processing; prognosis (key words)

I. INTRODUCTION

Bridge scour is the removal of sediments from around bridge pier, compromising the integrity of the structure [1]. It is estimated that 60% of all the bridge failures result from scour [2], and is the most common highway bridge failure in the United States, where 46 out of 86 major bridge failures during 1961 to 1976 were a result of scour near the piers [3]. Safety of the bridges (e.g. Custer Creek Bridge, Glanrhyd Creek Bridge, Schoharie Creek Bridge) was compromised due to scour caused by flash floods leaving the foundation of the piers vulnerable. Therefore, it is essential to ensure safety of bridges and predict the major scour event that may occur in the future. To forecast this event, a time dependent scour prognosis model is essential.

Many studies [4-8] have been carried out in order to understand the mechanism of scour around bridge piers. Many parameters such as velocity, flow depth, median particle size, pier diameter, gradation, type of soil (cohesive or non-cohesive) influence the scour evolution and as a result it is very difficult to formulate a mathematical model for scour prediction. Due to the complex nature of the scouring process, an inclusive theory for predicting the local scour around bridge piers was not achieved [9].

Empirical equations [6, 10-13] are widely used for predicting the scour depth at bridge piers. These equations differ from each other in the factors considered for constructing the model, laboratory / field conditions. The most commonly used equation is the Colorado State University equation recommended by the US Department of Transportation's Hydraulic Engineering Circular no. 18 (HEC-18) [14]. In 2001, a modified HEC-18 [15] equation was presented which had a correction factor (K4) for armoring by bed material size. In 2012 [16], the correction factor (K4) in the HEC-18 equation [15] was removed. Landers [17] evaluated selected empirical equations using 139 scour measurements in live-bed and clear water conditions. Their study indicates that none of the selected equations predict the scour depth accurately for all the measured conditions. Mueller [18] compared the scour equations using the data set collected by USGS [17]. The results of this study indicate better performance of HEC-18 equation compared to the other equations; however, it very frequently over-predicted the scour depth.

Soft computing techniques such as neural networks are being used for civil engineering applications [19-23]. Azamathulla et al. [20] presented the use of alternative neural networks to predict the scour below spillways. The results indicate that neuro-fuzzy scheme provides better estimates of the scour compared to empirical equations. This study was limited to predicting the scour depth in ski-jump type of spillways. Bateni et al. [22] presented a neural network methodology for predicting the scour depth around bridge piers. This methodology results in a more accurate scour depth compared to the empirical equations but do not provide the confidence intervals for the predictions. McIntosh [24] and Mueller et al. [25] showed that neural networks give better results when compared to empirical equations; however, a Neural Network (NN) model needs to set up different learning parameters, number of hidden layers, and the number of nodes in a particular hidden layer [20]. Also, large training sets are required to find the optimal values for the above parameters

and the NN model suffers from the problem of local minima. As the number of learning parameters increase, the objective function for optimization becomes higher dimensional, and as a result, the optimization process may yield to local minima. Support Vector Regression (SVR) has been used by researchers to predict the scour depth [9, 26-27]. These studies indicate that SVR gives accuracy between 25% and 40% for a scour depth of approximately 2m. These models still do not predict the time dependent scour.

There are only a few time-dependent scour models in the literature [8, 23, 28]. Mia et al. [8] developed a design method for predicting time dependent scour at cylindrical bridge piers. This study was limited to clear water scour under laboratory conditions. Bateni et al. (2007) [23] presented the use of Bayesian neural networks to predict the time-dependent scour in which both time-dependent and equilibrium scour depth were calculated. This study was solely performed on experimental laboratory datasets. Hong et al. [28] developed a SVR based approach to predict the time-dependent scour under different sediment conditions and was able to capture the physics of the scouring process by considering parameters such as actual and critical Froude number. All the methods described above are deterministic regression methods and hence do not provide the confidence with which the predictions are made. A scour depth predicted with unknown confidence can result in failure of the bridge structures. In these methods, the time-dependent scour is predicted at every time step, but the information of how the scour evolves over a given period of time into the future is not discussed.

In this paper, we use RFID based measurements to detect the current scour depth; and a prognosis methodology to predict the evolution of scour depth. More details about RFID system are presented in the next section. We investigate Gaussian Process (GP) [29-31], which is a probabilistic data driven approach, with Bayesian uncertainty for predicting the time-dependent scour. Using suitable combination of kernel functions, GP can accurately predict increasing and decreasing trends in the data. In a similar study on concentrations of CO_2 in the atmosphere, the robustness of GP in prediction of CO_2 concentrations, which increase and decrease due to seasonal changes, was reported by Rasmussen [31]. Scour depth is known to continually increase and decrease in case of live-bed scour due to erosion and re-filling of the sediment near bridge pier [25]. GP projects the nonlinear input-output mapping to a high dimensional space using kernel functions where the mapping becomes linear [31]. The applicability of GP is investigated for (i) predictions of the scour depth for a given set of flow conditions; and (ii) determination of the confidence intervals for the predicted scour depth.

II. RFID System

RFID is a wireless automated identification technology that utilizes radio frequency (RF) waves to transfer information between a reader and a transponder (short for transmitter and responder) via an antenna [32-33]. An important feature of the RFID technology is that a unique identification number can be assigned to each transponder, allowing different transponders within the system to be identified [32]. The system will be able to detect the orientation of the transponders along with their distance from the antenna based on the obtained signal strength. The main components of the RFID system shown in Fig. 1 are (i) antenna, which generates electromagnetic field, (ii) reader, which reads the signals (iii) transponders, which reflect the signal from the antenna. RF waves are transferred from a reader through an antenna to the transponders. The transponders are passive in nature, and reflect the received RF waves, which are transmitted back to the antenna. The level of degradation in the returned signal is related to the distance between the transponder and antenna.

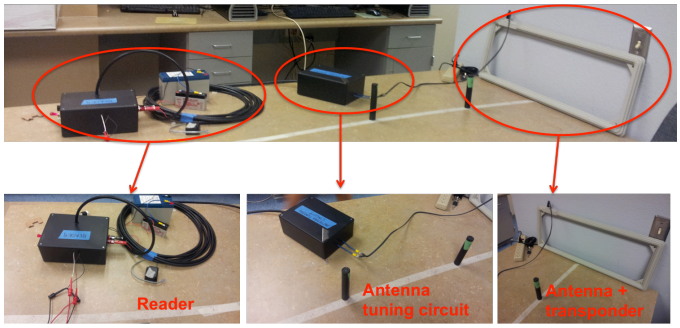

Fig. 1 RFID system with components (Texas Instruments Inc)

The antenna sends waves to each transponder at specific intervals of time and checks the level of degradation of the returned signal [32]. The information from all the transponders can be analyzed to evaluate the scour depth. Maximum signal strength is obtained when the axis of the transponder is perpendicular to the antenna. As the axis becomes parallel to the axis of the antenna, the signal strength decreases. This phenomenon can be used to measure the angle of the transponders with respect to the axis of the antenna [32]. As the scour happens, and the exposed transponder starts to rotate, the intensity of the returned signal reduces implying scour hole formation. Analyzing the signal from all the transponders and finding the number of transponders whose axis are parallel to the axis of antenna; the depth of scour hole can be estimated considering the change in the level of the signals from transponders. The advantage of using RFID technology is the capability to transfer scour data online to a central base station, where the prognostic algorithms are used to make predictions.

A. Field Test

Preliminary field tests were conducted by University of Iowa at Clear Creek Bridge near Camp Cardinal. Four transponders were buried under water at different depths and the data about signal strength decay was collected. The results indicated that the signal decay was approximately 50% for a distance of 2.75m, and the overall detection range for the antenna was 5m.

Further, the robustness of the RFID system for detection of scour was examined by installing a prototype of the system (as shown in Fig. 2) at the N Bush Highway Bridge in Arizona. In this field test, the data of signal strength degradation was collected. Since there was no scour at the bridge at the time of field test, the signal strength data was collected from different depths of transponder in the riverbed.

Fig. 3 shows a typical RFID sensor data. Data level 1 shows the charging of the transponder. Data level 2 shows the intensity of the returned signal. As the returned signal strength from the transponder decreases, the magnitude of data level 2 reduces. Data level 3 shows the synchronization stage of the transponder.

Fig. 2 Installing the RFID system near bridge pier

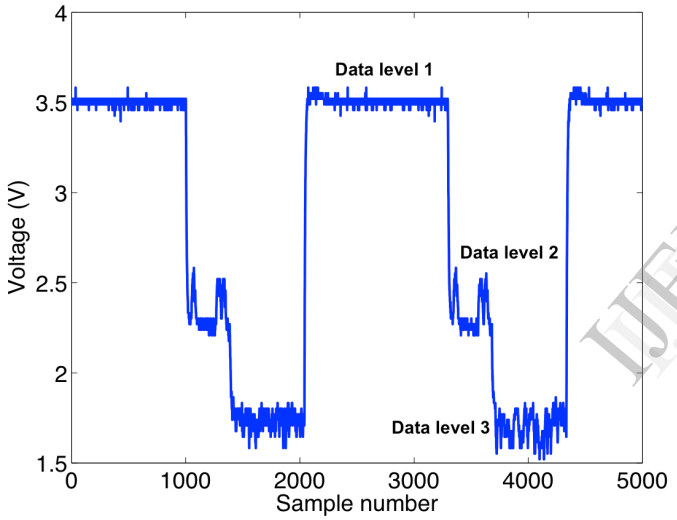

Fig. 3 Typical RFID signal

A smaller antenna (71cm x 27cm) with a detection distance of 1.2m was initially used for the field-testing. Having the data of signal degradation for different depths in soil and water, the scour depth can be estimated. Data was collected while the transponders were buried at different depths in water and soil. Fig. 4 shows the voltage level obtained when the transponder is buried in different media (water, soil). The curve corresponding to the legend "Water (big antenna)" in Fig. 4 was obtained from the experiments conducted in University of Iowa. The y-axis in Fig. 4 shows the percentage decay in the original voltage (when the transponder is at 0cm from the antenna). It is to be noted that, for this particular field test, the variation of voltage was the important factor, rather than the overall detection distance. Since a smaller antenna was used, the detection distance is 1.2m. The signal strength decay in different media was the main goal for installing this prototype antenna.

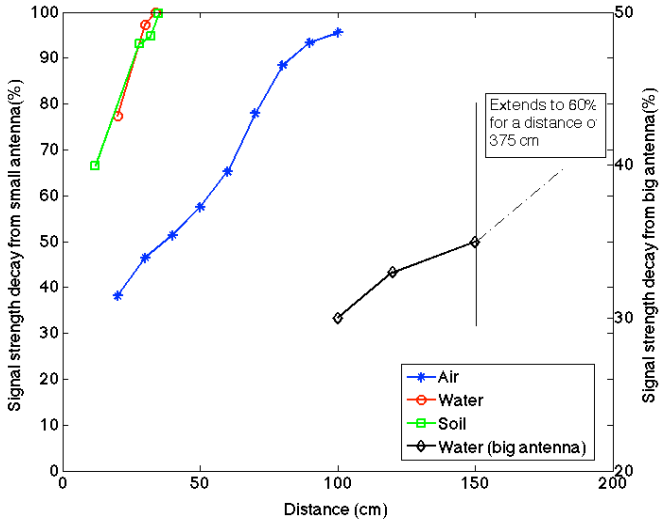

Fig. 4 Signal strength decay in different media.

A larger antenna (diameter 1.1m), developed at adaptive intelligent materials and systems center at Arizona State University, as shown in Fig. 5 with a detection range of 9m was built and installed at New River Bridge in Arizona. Increasing dimensions of the antenna generates a larger electromagnetic field.

Along with the RFID system, a pressure transducer was used to measure the approach flow depth. The velocity of the flow can be computed from the flow depth by using the Manning equation [34]. As there was no scour during the data collection process, the temporal scour data was not available to be collected. The scour depth collected from RFID, flow depth, and velocity of the flow at a given instant of time are the input parameters for the predicting scour using the proposed prognosis model which is explained in the next section.

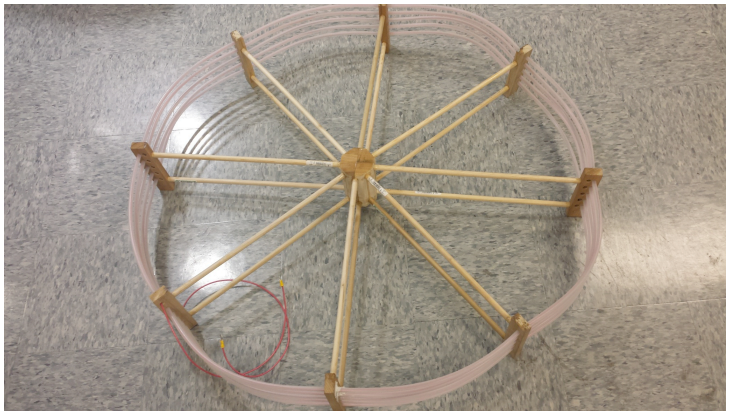

Fig. 5 Large size antenna (diameter 1.1m)

III. PARAMETERS AND DATA SETS

The critical scour depth (d_c) depends on various parameters, the most important of which are velocity of the flow (V), flow depth (h), skew (S_k), pier diameter (D), median

particle size (d_{50}), and gradation (σ) [25]. The relationship between these parameters and scour depth can be written in the form:

$$d_c = f(h, V, S_k, D, d_{50}, \sigma) \quad (1)$$

The type of evolution of the scour changes with different characteristics of the input parameters. The parameters D, S_k, d_{50}, and σ will almost remain the same for any particular location in the streambed (near the bridge pier). Hence, in order to study the temporal evolution of the scour for a particular bridge, the model can be simplified by removing these parameters, as they remain almost constant over the given period of time. This gives a simple yet robust model for predicting the time-dependent scour depth, which will be discussed in the subsequent section. The relationship for the scour depth (d) as a function of time (t) can be written in the form:

$$d(t) = f(h, V, t), \quad (2)$$

As there was no scour occurring at the New River Bridge, the temporal scour data was not available at the time of this study. Therefore, datasets from the literature were used to validate the proposed prognosis model. It is to be noted that the input parameters; current scour depth, flow depth and velocity are obtained through the RFID system and pressure transducer as mentioned in the previous section.

In this study, two data sets were used to validate the GP prognosis model.

(i) A laboratory dataset [35] that contained 84 data points from experiments conducted in four different flumes was used. The characteristics of the dataset are shown in Table 1. The minimum value of the parameter is x_{min}, maximum x_{max}, mean x_{mean}, standard deviation x_{std}, variation coefficient C_{vx}, and skewness coefficient S_x.

(ii) The field dataset availabl in the bridge scour management system [25] containing 493 pier scour measurements was used for this study. The dataset has pier scour measurements at 79 different test sites in 17 states in the US. The characteristics of this dataset are shown in Table 2.

Table 1
Characteristics of the laboratory dataset [35]

Variables	x_{min}	x_{max}	x_{mean}	x_{std}	C_{vx}	S_x
D (mm)	16	200	85.0075	48.2872	0.568	0.7229
d_{50} (mm)	0.8	7.8	1.9261	1.7819	0.9252	1.9797
h (mm)	20	600	269.7262	210.4478	0.7802	0.7385
V (m/s)	0.165	1.208	0.4251	0.2698	0.6346	1.3352
t (min)	200	15000	3909.3	3096.9	0.7922	1.9316
d (mm)	4	318	122.75	88.744	0.723	0.5961

Table 2
Characteristics of the field dataset [25]

Variables	x_{min}	x_{max}	x_{mean}	x_{std}	C_{vx}	S_x
D (m)	0.9	5.5	1.9152	1.4753	0.7703	1.0905
d_{50} (mm)	0.48	0.74	0.6642	0.0978	0.1473	-1.2947
h (m)	4.3	15.4	7.0848	3.1021	0.4378	1.3501
V (m/s)	0	2.3	0.8894	0.4766	0.5358	0.5407
t (days)	1	127	33.5	40.5945	1.2118	1.2238
d (m)	0.2	4.6	1.2985	1.3474	1.0377	1.4195

IV. GAUSSIAN PROCESS PROGNOSIS MODEL

A GP model, which includes Bayesian uncertainty, is used for the prediction of the time-dependent scour depth. The GP is a collection of random variables, any finite number of which have a joint Gaussian distribution. GP makes predictions by projecting the input space to the output space, through inferring their underlying non-linear relationship [31]. Once the algorithm is trained with the input and output parameters, it can predict the output parameter for unknown or new sets of input parameters. The input and output space for the GP in the current scour prediction problem are shown below in the form of matrices.

$$\text{Input space} = \begin{bmatrix} h_1 & V_1 & t_1 \\ h_2 & V_2 & t_2 \\ . & . & . \\ . & . & . \\ . & . & . \\ h_t & V_t & t_t \end{bmatrix}$$

$$\text{Output space} = \begin{bmatrix} d_1 \\ d_2 \\ d_3 \\ . \\ . \\ d_t \end{bmatrix}$$

The posterior distribution over the predicted scour depth at time "t" (d_t) can be written as:

$$f(d_t \mid T, K_t(x_i, x_j), \theta) = \frac{1}{Z}\exp\left(-\frac{d_t - \mu_{d_t}}{2\sigma_{d_t}^2}\right); \; i, j = 1, \ldots, t\text{-}1 \quad (3)$$

where Z is a normalizing constant, T = $\{x_i, d_i\}_{i=1}^{t}$ is the training set in which x_i is a vector of input variables and d_i is the output variable, K is the kernel / covariance matrix, $\boldsymbol{\theta}$ is the set of hyper-parameters, μ_{d_t} is the mean, and $\sigma_{d_t}^2$ is the variance of the distribution, which is related to the error in the prediction. The error is attributed to the training of GP under varying conditions. The kernel function transforms the non-linear parameters to a high dimensional space where they are linearly separable. Even though the assumption of Gaussian distribution is made on each variable, the results show that it is a good assumption for this application. It is necessary to verify the effect of using different kernel functions to select the best kernel function for this application. Squared Exponential (SE) and Rational Quadratic (RQ) kernel functions are considered in this study.

The SE kernel is expressed as [31]:

$$K_{se}(x_i, x_j) = \theta_1^2 \exp\left(-\frac{(x_i - x_j)^2}{\theta_2^2}\right), \qquad (4)$$

where θ_1 and θ_2 are the hyper-parameters which govern the accuracy of the predicted values. The RQ kernel has three hyper-parameters and is expressed as [31]:

$$K_{rq}(x_i, x_j) = \theta_3^2 \left(1 + \frac{(x_i - x_j)^2}{2\theta_4 \theta_5^2}\right)^{-\theta_4}, \qquad (5)$$

where θ_3, θ_4 and θ_5 are the hyper-parameters. The hyper-parameters are first initialized to a reasonable value, and their optimum value is found by minimizing the negative log marginal likelihood (L) given by [31]:

$$L = -\frac{1}{2}\log|K_t| - \frac{1}{2} d_t^T K_t d_t - \frac{t}{2}\log 2\pi \qquad (6)$$

The number of parameters in the optimization space influences the initial values for the HPs. If there are 2 HPs, the initial value does not affect the optimization routine. The following analysis shows that for 5 HPs, the HPs should be initialized between 0.1 and 1. A reasonable value for t

he HPs in scour problem is recommended to be 0.1 and the data should be normalized. The kernel function is evaluated using the initialized hyper-parameters. The optimal values for the hyper-parameters are found by using the conjugate gradient descent optimization algorithm [36] through considering "*L*" as the objective function to be minimized. The training set is updated progressively within time (as new data is available) to (i) improve the accuracy of prediction, and (ii) ensure that the model will be able to capture global and local variations in the parameters.

Table 3 shows the details of the kernel functions used, initialized HPs, optimal HPs and optimal function (L) value. When the SE kernel function is used and the HPs are initialized to (0.1,0.1), the optimal function value is found to be -43.46. Even if the HPs are initialized to (1,1) and (10,10), the same optimal value for the objective function is achieved. With two HPs, the optimization space is 3-dimensional, and the gradient descent algorithm can easily find the optimal descent direction.

The laboratory dataset shown in section 2 was chosen for illustrating the effect of different kernel functions on optimization of HPs. When a sum of both SE and RQ kernel functions [31] is used and all the HPs are optimized to a value of 0.1, an objective function value of -43.46 is achieved, which is almost equal to the value achieved using a SE kernel function. When all the HPs are initialized to a value of 1, the objective function value is -43.51, which is close to -43.46. But when the HPs are initialized to a value of 10, due to the higher dimensionality, the algorithm gets stuck in local optima and doesn't proceed further. Here the optimum function value obtained is +0.0556.

Table 3
Initialized HPs and their optimum values with different kernel functions

Kernel Function	Initialized hyper-parameters (θ)	Optimum hyper-parameters (θ_{opt})	Optimum function (L) value
SE	(0.1,0.1)	(-2.09, -2.53)	-43.4612
SE	(1,1)	(-2.09, -2.53)	-43.4612
SE	(10,10)	(-2.09, -2.53)	-43.4612
SE + RQ	(0.1,0.1,0.1,0.1,0.1)	(-0.87, -4.61, -2.05, -2.51, 2.00)	-43.4625
SE + RQ	(1,1,1,1,1)	(-2.04, -2.48, -3.81, -6.34, 0.44)	-43.5141
SE + RQ	(10,10,10,10,10)	(10.02, 9.93, 10.02, 9.98, 10.02)	0.0556

Fig. 6 shows the number of iterations to achieve the optimum value for the scenarios discussed earlier. When the HPs are initialized to (0.1,0.1) and (1,1) using the SE kernel function, the convergence is obtained in 28 and 29 iterations, respectively. However, when the HPs are initialized to (10,10) the convergence is obtained after 38 iterations. When the HPs are initialized to (1,1,1,1,1) using a sum of SE and RQ kernel functions, the convergence is obtained in 28 iterations. The SE kernel function was found to be working well and was used in the further analysis. It is to be noted that the HPs are not constant for a particular scour data set, and they depend on the outcome of the optimization process. The HPs should be initialized to the value mentioned above, and the algorithm based on the training sets will automatically calculate the optimum values of the HPs.

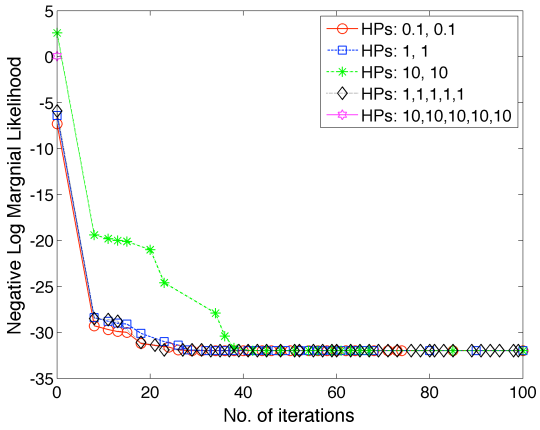

Fig. 6 Optimization of hyper-parameters with different kernel functions

V. RESULTS AND DISCUSSION

A. Laboratory Dataset

The data for training was chosen such that the evolution of the scour as a function of time could be predicted. All the data was normalized before the analysis to ensure that all the parameters are equally weighted. As the total data was normalized, the HPs in equation (4) were initialized to θ_1 = 0.1, θ_2= 0.1, and the SE kernel function was used. In all the following results, the predictions were made at each time step till the next time step at which the measurement is available.

Three different cases were selected to show the adaptability and robustness of the developed algorithm. In the first case the data from an abrupt change in the scour depth was included. The second case demonstrates the increasing accuracy of the algorithm with increasing training data. The third case demonstrates the predictive capability of the algorithm under equilibrium scour conditions. Instead of using a fixed set of training and testing data, as the training data is dynamically updated with the current measurement after every iteration, more points can be used for testing and training. This process improves the prediction accuracy because we always consider current measurement before making predictions. Table 4 shows the dynamic measurement updating.

Fig. 7 shows the predicted normalized scour depth and the associated error in prediction as a function of time. The shaded region in Fig. 7 is the 95% confidence interval (2 standard deviations) for the prediction. The gradient shows confidence interval changing from 95 to 100%, as it gets closer to the predicted scour depth. The legend "Confidence interval (upper) indicates the gradient above the predicted scour depth, and the legend "Confidence interval (lower) indicates the gradient below the predicted scour depth. The algorithm is able to predict the scour depth accurately within an error of less than 5% for almost the entire scour evolution regime. The error of 8% at the final point of prediction is the result of limited training data set. The information about the change after a continuously steady scour depth was not available in the training dataset. However, as more data becomes available about the change, the algorithm predicts the scour depth accurately. Fig. 8 (case 2) shows this phenomenon, where the model is updated dynamically to get accurate results. The first prediction in Fig. 8 is based on three training data points leading to a lower confidence level; however, as the training set is updated by iteration, the error reduces significantly. These results show the algorithm's ability to adapt as it receives more training data.

Table 4
Example of dynamic measurement updating scheme

Time index (t)	Training data points	Testing data point
t=1	1 to 3	4
t=2	1 to 4	5
t=3	1 to 5	6
t=4	1 to 6	7

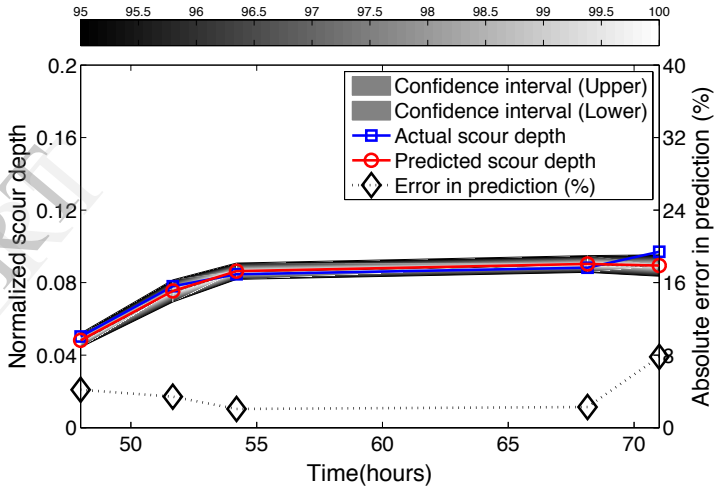

Fig. 7 Prediction under insufficient data about abrupt change in scour depth (Case 1)

Fig. 9 (case 3) shows the plot of the predicted scour-depth with time in a different flume [35]. This data was chosen to show the equilibrium scour depth. In this case, the equilibrium scour depth is achieved after 91 hours. Once the equilibrium scour depth is achieved, the scour remains almost constant and does not change with the input parameters. Fig. 9 shows the capability of the algorithm to capture this phenomenon. During the equilibrium phase, the error in prediction is less than 2%.

The above three cases show the adaptability and robustness of the GP algorithm under different conditions. Fig. 10 shows the plot of the actual scour versus predicted scour for all the dataset. Out of the 84 points in the dataset, 27 points that were chosen from different flumes under different flow conditions were used for prediction. Fig. 10 shows almost 50% of the points are predicted with an error of less than 5% even with limited training data points, unlike other deterministic regression methods [9].

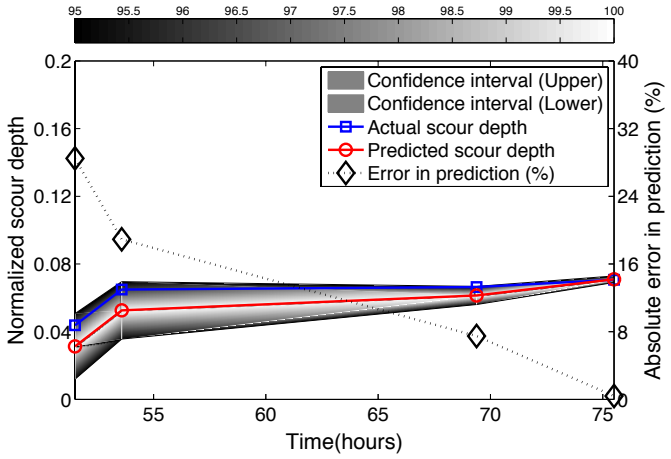

Fig. 8 Prediction with increasing training data (Case 2)

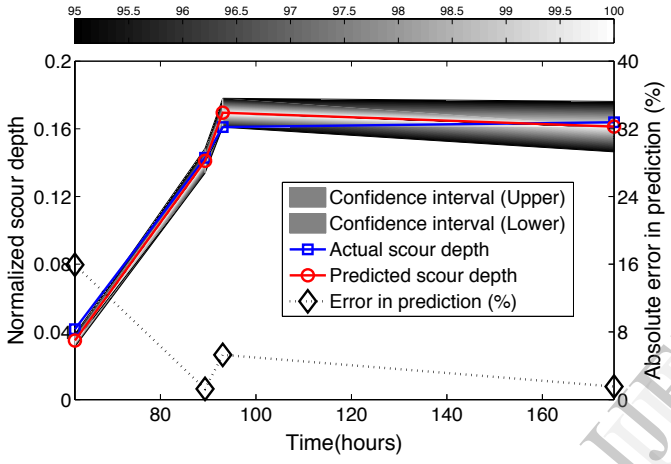

Fig. 9 Prediction under equilibrium scour conditions (Case 3)

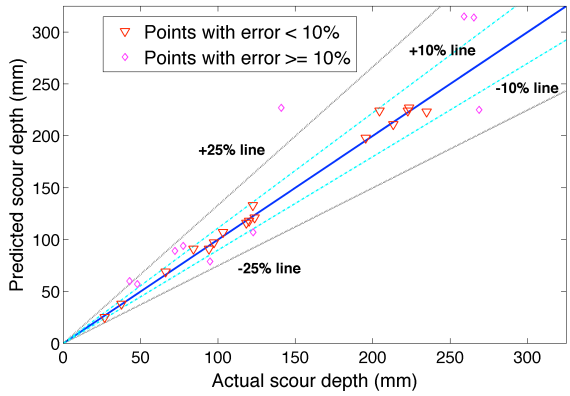

Fig. 10 Actual scour vs. predicted scour for laboratory dataset

Results show that 92.5% of the points are predicted with an error of less than or equal to 25%. Out of these points, which had the error in between 10% and 25%, are the points that had the least amount of training data (≤ 4 training data points). The increase in the number of training points increases the accuracy of scour prediction as shown in Fig. 7. A coefficient of determination of 0.9821 was achieved for the training set and a value of 0.9016 was achieved for the test data.

B. Field Dataset

Out of the 493 pier scour measurements available in the bridge scour data management system [25], 66 data points were carefully chosen for further analysis. These were selected based on the availability of continuous time scour data. Out of the 79 test sites, only 9 sites had frequent continuous time scour data, which can be used for the analysis. Those bridges, which had data collected approximately every month, was used for analysis. The 66 data points were collected in different locations under different flow conditions to ensure variability in the parameters. Of the 66 data points, 30 data points were used for testing the algorithm.

Fig. 11 shows the prediction of time dependent scour for a bridge in Montana [25]. The pier at which the scour measurements were made is a square pier. The bed material was non-cohesive and the effect of debris was insignificant. The GP algorithm is able to predict the scour depth with an error of less than 10%. The algorithm was then examined for a bridge with round piers located in Virginia [25]. The bed-material and the debris effect were unknown for this location. The time dependent scour data was available for a period of 120 days. Fig. 12 shows the prediction of the scour with time. The scour depth is predicted within an error of less than 15% for most of the time regime. The next dataset was chosen so that it shows continuous increasing and decreasing of scour depth with time. The third bridge is located in Virginia and the bed material and debris effects were unknown [25]. Fig. 13 shows the prediction under these conditions. The algorithm is able to capture the trend of increasing and decreasing scour depth with an error of less than 25% for most of the time regime.

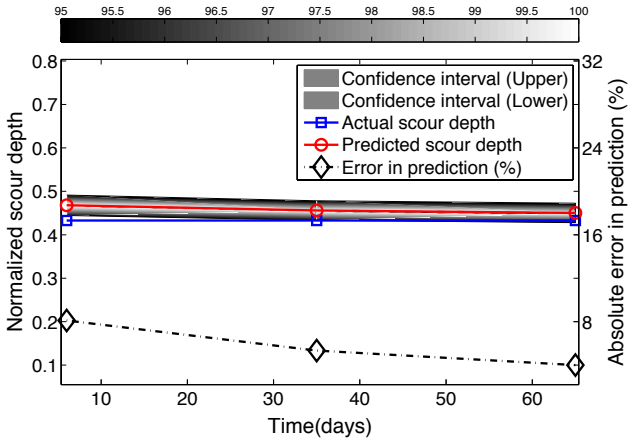

Fig. 11 Prediction of scour depth with non-cohesive soil and insignificant debris

Fig. 14 shows the plot of actual scour depth versus predicted scour depth for the complete dataset. All the predicted scour depths, except two, lie in between the ±25% lines.

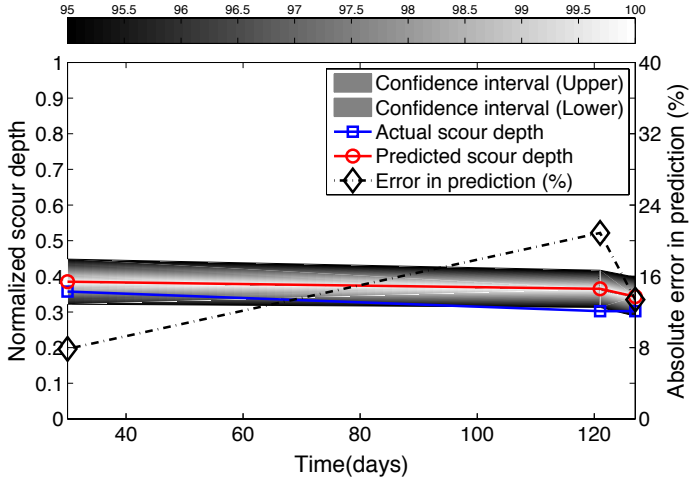

Fig. 12 Prediction of scour depth with unknown soil type

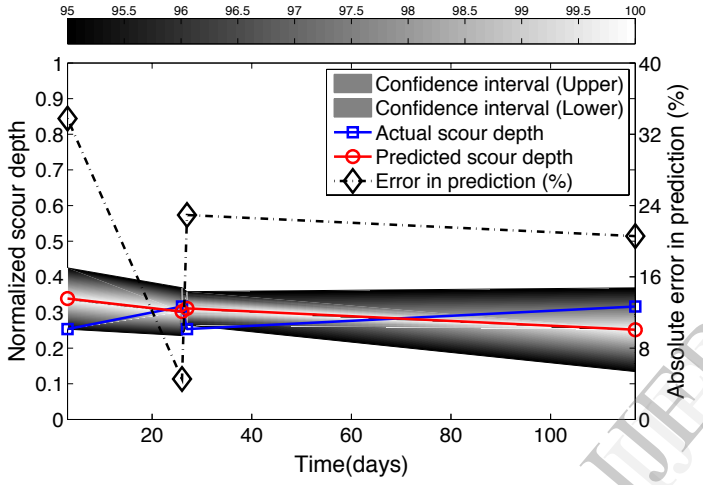

Fig. 13 Prediction of continually varying scour depth

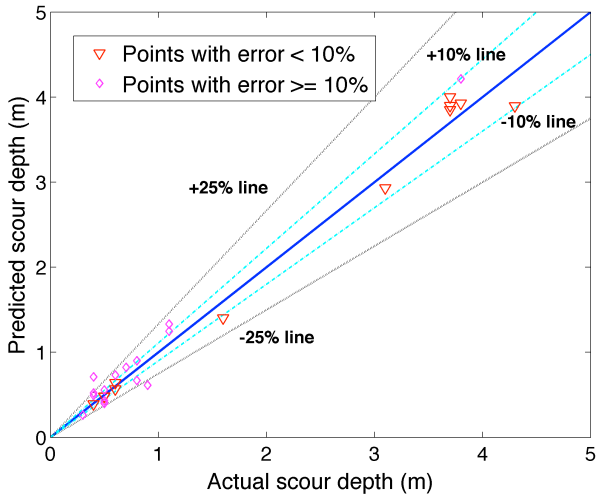

Fig. 14 Actual scour vs. predicted scour for field dataset

In all the above cases, the predictions were made with a very limited training dataset. The algorithm is able to predict the scour depth with an error of less than 25% for most of the cases.

VI. CONCLUSIONS

The applicability of probabilistic Gaussian process based algorithm for accurate and efficient prediction of the time-dependent scour has been investigated. Scour depth, flow depth and velocity are the critical input parameters for the prognosis model. RFID system is used to measure the scour depth at a given instant of time. The velocity and flow depth are calculated using the data from pressure transducer and Manning equation. These sensors were installed at New River Bridge in Arizona. Since, there was no scour happening at the time of this study, data from literature was used to validate the proposed algorithm. The effect of hyper-parameter initialization on the convergence of the algorithm was examined. Three different scenarios were demonstrated to test the robustness of the algorithm. In the first case, the data containing a sudden increase in scour was considered. The algorithm was able to predict this phenomenon with an error of 8%. In the second case, the adaptability of the algorithm with increasing training data is shown. The error in the prediction decreases asymptotically as more training data becomes available. In the third case, the data was chosen such that the scour has reached the equilibrium value where it doesn't change with the varying input conditions. The GP algorithm captured this phenomenon and predicted a constant scour depth during this period. Out of the 84 data points available, 27 data points were used for testing the algorithm. A coefficient of determination of 0.9821 was achieved for the training data and a value of 0.9016 was achieved for the testing set. The algorithm was also validated using field dataset from the literature. This dataset had the data of continually increasing and decreasing scour depth. Out of the 66 available data points, 30 were used for testing the algorithm. A coefficient of determination of 0.9018 was achieved for testing data and a value of 0.9715 was achieved for the training dataset. The developed GP algorithm improved the accuracy of scour prediction considerably.

ACKNOWLEDGMENT

"This project is supported by Grant No. RITARS-12-H-ASU from the DOT Research and Innovative Technology Administration (RITA). The authors also would like to acknowledge the guidance and contributions of Mr. Caesar Singh, the Program Manager at the DOT."

We would also like to thank Dr. Itty P. Itty, head of the hydraulics section at Arizona Department of Transportation, Dr. Bing Zhao, engineering application division river mechanics branch manager and Mr. Amir Motamedi hydrology/hydraulics branch manager at Flood Control District of Maricopa County for their valuable suggestions.

We would like to thank Dr. Thanos Papanicolaou, from the department of civil and environmental engineering at the University of Tennessee for providing RFID components and valuable suggestions.

"DISCLAIMER: The views, opinions, findings and conclusions reflected in this paper are the responsibilities of the authors only and do not represent the official policy or position of the USDOT/RITA, or any State or other entity."

REFERENCES

[1] Warren, LP. (2011). "Scour at Bridges: Stream Stability and Scour Assessment at Bridges in Massachusetts." *U.S. Geological Survey*, 2011.

[2] Landers, M. N. (1992). "Bridge Scour Data Management." *Proceedings of the Hydraulic Engineering sessions at Water Forum '92*. Baltimore, Maryland.

[3] "USGS OGW, BG: Using Surface Geophysics for Bridge Scour Detection". Water.usgs.gov. Retrieved 2010-07-30.

[4] Ettema, R., Melville, B. and Barkdoll, B. (2001). "Scale effect in pier-scour experiments." *Journal of Hydraulics Engineering*, 124(6), 639-642.

[5] Lim, SY. and Cheng, NS. (1998). "Prediction of live-bed scour at bridge abutments." *Journal of Hydraulics Engineering*, 124, 635-642.

[6] Melville, B. W., and Sutherland, A. J. **(**1988**).** "Design method for local scour at bridge piers." *Journal of Hydraulics Engineering*, 114(10), 1210–1226.

[7] Melville, B. (1997). "Pier and abutment scour: integrated approach." *Journal of Hydraulics Engineering*, 123, 125-136.

[8] Mia, F. and Nago, H. (2003). "Design method of time dependent local scour at circular bridge pier." *Journal of Hydraulics Engineering*, 129(6), 420-427.

[9] Pal, M., Singh, N.K. and Tiwari, N.K. (2011). "Support vector regression based modeling of pier scour using field data." *Engineering Applications of Artificial intelligence*, 24(5), 911-916.

[10] Froehlich, D. C. (1989). "Local scour at bridge abutments." *Proceedings of the National Conference on Hydraulic Engineering*, New York, 13–18.

[11] Melville, B. W. **(**1992**)**. "Local scour at bridge abutments." *Journal of Hydraulics Engineering*, 118**(4),** 615–631.

[12] Abed, L., and Gasser, M. M. **(**1993). "Model study of local scour downstream bridge piers." *Proceedings of the National Conference on Hydraulic Engineering*, San Francisco, 1738–1743.

[13] Richardson, J. R., and Richardson, E. V. **(**1994**). "**Practical method for scour prediction at bridge piers." *Proceedings of the ASCE National Conference on Hydraulic Engineering*, Buffalo, N.Y., 1–5.

[14] Federal Highway Administration, **(**1993**)**. "Evaluating scour at bridges, Hydraulic Engineering Circular No. 18, Rep. No. FHWA-IP-90-017." *Federal Highway Administration (FHWA)*, U.S. Department of Transportation, Washington, D.C

[15] Federal Highway Administration, **(**2001**)**. "Evaluating scour at bridges, Hydraulic Engineering Circular No. 18, Rep. No. FHWA-NHI-01-001." *Federal Highway Administration (FHWA)*, U.S. Department of Transportation, Washington, D.C

[16] Federal Highway Administration, **(**2012**)**. "Evaluating scour at bridges, Hydraulic Engineering Circular No. 18, Rep. No. FHWA-HIF-12-003." *Federal Highway Administration (FHWA)*, U.S. Department of Transportation, Washington, D.C

[17] Landers, M. N., Mueller, D. S., and Richardson, E. V. **(**1999**). "**U.S. Geological Survey field measurements of pier scour." *ASCE compendium, stream stability and scour at bridges*, Richardson, E., and Lagasse, P., eds., ASCE, Reston, VA.

[18] Mueller, D. S. **(**1996**). "**Local scour at bridge piers in nonuniform sediment under dynamic conditions." Ph.D. thesis, *Colorado State University*, Fort Collins, Colorado.

[19] Jiang, X. and Adeli, H. (2004). "Clustering-Neural Network Models for Freeway Work Zone Capacity Estimation." *International Journal of Neural Systems*, 14(3), 147-163

[20] Azamathulla, H.Md., Deo, M.C. and Deolalikar, P.B. (2008). "Alternative neural networks to estimate the scour below spillways." *Advances in Engineering Software*, 39(8), 689-798.

[21] Firat, M. and Gungor, M. (2009). "Generalized regression neural networks and feed forward neural networks for prediction of scour depth around bridge piers." *Advances in Engineering Software*, 40(8), 731-737.

[22] Bateni, S., Borghei, S. and Jeng, D. (2007). "Neural network and neuro fuzzy assessments for scour depth around bridge piers." *Engineering Applications of Artificial Intelligence*, 20(3), 401-414.

[23] Bateni, S., Jeng, D. and Melville, B. (2007). "Bayesian neural networks for prediction of equilibrium and time-dependent scour depth around bridge piers." *Advances in Engineering Software*, 38(2), 102-111.

[24] McIntosh, J.L. (1989). "Use of scour prediction formulae." Proceedings of the Bridge Scour Symposium, McLean, VA, *Federal Highway Administration Research Report FHWA-RD-90-035*, 78-100.

[25] Mueller, D. and Wagner, C. (2005). "Field Observations and Evaluations of Streambed Scour at Bridges." *Federal Highway Administration*, US Department of Transportation, publication no. FHWA-RD-03-052.

[26] Goel, A. and Pal, M. (2009). "Application of support vector machines in scour prediction on grade-control structures." *Engineering Applications of Artificial Intelligence*, 22, 216–223.

[27] Nassar M. A., Ibrahim, A,A. and Negm, A,M. (2009). "Modeling local scour downstream of hydraulic structures using support vector machines (SVMs)." *Proceedings of the 6th international conference on Environmental Hydrology and 1st symposium on Costal and Port Engineering*, 28-30 September 2009, ASCE-ES, Cairo.

[28] Hong, J., Goyal, M., Chiew, Y. and Chua, L. (2012). "Predicting time-dependent pier scour depth with support vector regression." *Journal of Hydrology*, 468-469, 241-248.

[29] Gibbs, M. N. (1997). "Bayesian Gaussian Processes for Regression and Classification." PhD Thesis, *Univ. of Cambridge*, Cambridge, England, U.K.

[30] MacKay, D. (2003). "Information Theory, Inference, and Learning Algorithms." *Cambridge Univ. Press*, Cambridge, England, U.K.

[31] Rasmussen, C.E. and Williams, C.K.I. (2006). "Gaussian processes for machine learning." *The MIT Press*, Cambridge, MA.

[32] Papanicolaou, AN., Elhakeem, M. and Tsakiris, A. (2010). "Autonomous Measurements of Bridge Pier and Abutment Scour Using Motion-Sensing Radio Transmitter." *Transportation Research Board*, Report No. TR-595. 2010.

[33] Lauth, T. J. and Papanicolaou, A. N. (2008). "Experimental/Feasibility Study of Radio Frequency Tracers for Monitoring Sediment Transport and Scour around Bridges." In *World Environmental and Water Resources Congress* (pp. 12-16).

[34] Manning R. (1891). "On the flow of water in open channels and pipes". *Transactions of the Institution of Civil Engineers of Ireland*, 20, 161-207.

[35] Melville, B. and Chiew, Y. (1999). "Time scale for local scour at bridge piers." *Journal of Hydraulic Engineering*, 125(1), 59-65.

[36] Hestenes, M R. and Stiefel, E (1952). "Methods of Conjugate Gradients for Solving Linear Systems." *Journal of Research of the National Bureau of Standards*, 49(6), 409-436.